ANTIOXIDANTS & REDOX SIGNALING
Volume 9, Number 9, 2007
© Mary Ann Liebert, Inc.
DOI: 10.1089/ars.2007.1660

Forum Original Research Communication

Contribution of Lysosomal Vesicles to the Formation of Lipid Raft Redox Signaling Platforms in Endothelial Cells

SI JIN, FAN YI, and PIN-LAN LI

ABSTRACT

We have demonstrated that the formation of lipid raft (LR)-redox signaling platforms membrane is associated with activation of acid sphingomyelinase (ASMase) in coronary arterial endothelial cells (CAECs). Given that the trafficking of lysosomal vesicles might play an essential role in ASMase activation, the present study tested whether lysosomal vesicles contribute to the formation of LR redox signaling platforms. By confocal microscopy, we found that Fas ligand (FasL) induced the formation of LR clusters in the plasma membrane of CAECs, accompanied by aggregation of NAD(P)H oxidase subunits, gp91^{phox} and p47^{phox}, and ROS production. When the cells were pretreated with two structurally different lysosomal vesicle function inhibitors, bafilomycin A1 (Baf) and glycyl-L-phenylalanine-β-naphthylamide (GPN), the FasL-induced LRs clustering was substantially blocked, and corresponding ROS production significantly decreased. By confocal microscopic observations in living CAECs by using LysoTracker, a colocalization of LRs and lysosomal vesicles was found around the cell membrane, which was abolished by Baf or GPN. Functionally, FasL-induced inhibition of endothelium-dependent vasorelaxation was also reduced by both inhibitors of lysosome function. These results suggest that lysosomal vesicles importantly contribute to the formation of LR-redox signaling platforms and thereby participate in the oxidative injury of endothelial function during activation of death receptor-Fas in coronary arteries. *Antioxid. Redox Signal.* 9, 1417–1426.

Lipid rafts (LRs) consist of dynamic assemblies of cholesterol and sphingolipids such as sphingomyelin (SM), ceramide, glycosphingolipids, and gangliosides as well as some phospholipids (2). Recently, increasing evidence exists that LRs clustering as a general mechanism plays an essential role in the initiation of receptor-mediated transmembrane cell signal transduction in a variety of mammalian cells such as lymphocytes, epithelial cells, neurons, and endothelial cells (9, 14, 16, 28). This LRs clustering-associated signaling mechanism is now considered a novel model that transduces and amplifies the signals generated by activation of different receptors such as death receptors, insulin receptors, some neurotransmitter receptors, and growth-factor receptors (2). By facilitating or amplifying transmembrane signaling, LRs clustering in the cell membrane could regulate various cell or organ functions or cellular activities such as cell proliferation, differentiation and apoptosis, T-cell activation, tumor metastasis, and neutrophil or monocyte infiltration and infection, and so on (2).

In recent studies, we reported that LRs clustering on the arterial endothelium recruited or aggregated some redox signaling molecules such as NAD(P)H oxidase subunits and Rac GTPase. The aggregation of these redox signaling molecules activated and enhanced production of superoxide ($O_2^{\cdot -}$) or reactive oxygen species (ROS) and thereby impaired endothelial function. This LRs clustering with redox signaling molecules was referred as to the formation of LR redox signaling platforms (32). It has been demonstrated that these signaling platforms in the membranes of coronary arterial endothelial cells (CAECs) are characterized by gp91^{phox} aggregation, p47^{phox} recruitment or translocation, and by activation of acid sphin-

[1]Department of Pharmacology & Toxicology, Medical College of Virginia Campus, Virginia Commonwealth University, Richmond, Virginia.

gomyelinase (ASMase) and subsequent production of ceramide. The production of ceramide in the cell membrane may form ceramide-enriched microdomains, which are able to fuse spontaneously to one or a few large macrodomains: clusters or platforms (15). However, it remains unclear how ASMases are recruited and activated in these LR platforms.

In previous studies, the rapid activation and translocation of ASMases into LRs were observed in response to various stimuli such as FasL, TNF-α and endostatin (2, 32). However, it remains unknown where these ASMase molecules come from. Although it has been reported that the ASMase gene gives rise to a common mannosylated precursor protein, SMase precursor-mannose, this gene product is shuttled into either the lysosomal trafficking pathway mediated by sortilin and mannose 6-phosphate receptor (19) or a secretory pathway (27). Given evidence that the activated form of ASMase localizes at the outer leaflet of the cell membrane (12), it seems that lysosome-associated vesicle transportation or trafficking of ASMase from the abluminal compartment to the cell membrane is a prerequisite for ASMase activation in the process of LRs clustering. The present study was designed to test this hypothesis to demonstrate that lysosomal ASMase contributes to the formation of LR redox signaling platforms. More specifically, when endothelial cells (ECs) are stimulated by death-receptor agonists such as FasL or CD95 antibody and TNF-α, lysosomal vesicles will traffic and migrate into the cell membrane, enriching ASMase locally. These SMases hydrolyze SM to produce ceramide and lead to the formation of ceramide-enriched macrodomains or LR platforms, which cluster or recruit NAD(P)H oxidase subunits, increase $O_2^{\cdot -}$ production, and ultimately result in endothelial dysfunction. To our knowledge, our results provide the first direct evidence supporting the view that lysosome-like vesicles are importantly involved in the formation of endothelial LR redox signaling platforms.

MATERIALS AND METHODS

Cell culture

Fresh bovine hearts were obtained from a local abattoir and immediately transported to our laboratory. The epicardial circumflex and anterior descending coronary arteries were quickly dissected and placed in RPMI 1640 supplemented with 5% fetal calf serum (FCS), 2% antibiotic–antimycotic solution, 0.3% gentamycin, and 0.3% nystatin and cleaned of surrounding adherent fat and connective tissue. The lumen of arterial segments was filled with 0.25% collagenase A in RPMI 1640 supplemented with 0.1% bovine serum albumin (BSA) and incubated at 37°C for 15–30 min. The arteries were then flushed with RPMI 1640 supplemented with 2% antibiotic–antimycotic solution, 0.3% gentamycin, and 0.3% nystatin. Detached bovine CAECs were collected and maintained in RPMI 1640 supplemented with 20% FCS, 1% glutamine, and 1% antibiotic–antimycotic solution at 37°C in 5% CO_2. Isolated bovine CAECs were identified by morphologic appearance (*i.e.,* cobblestone array) and by positive staining for von Willebrand factor antigen. All biochemical studies were performed by using CAECs of two to four passages.

Confocal analysis of LR clusters in CAECs

Individual LRs are too small (~50 nm) to be resolved by standard light microscopy; however, if raft components are crosslinked in living cells, clustered raft protein and lipid components can be visualized by fluorescence microscopy. For microscopic detection of LR platforms, CAECs were grown on glass coverslips and then treated with 10 ng/ml FasL (Upstate-Millipore, Billerica, MA) for 15 min to induce clustering of lipid rafts. In additional groups of cells, bafilomycin A1 (Sigma, St. Louis, MO; Baf, 100 n*M*) and glycyl-L-phenylalanine-β-naphthylamide (Sigma; MO, GPN, 100 μM) were added to pretreat the cells for 15 min before FasL stimulation. These cells were then washed in cold PBS and fixed for 10 min in 4% paraformaldehyde (PFA) in PBS and blocked with 1% BSA in TBS for 30 min. G_{M1} gangliosides enriched in LRs were stained by Alexa488-labeled cholera toxin B (alexa488-CTX, 1 μg/ml, 45 min) (Molecular Probes, Eugene, OR). Cells were extensively washed in cold PBS, fixed in 4% PFA for another 10 min, and mounted on glass slide with Vectashield mounting media (Vector Laboratories, Inc., Burlingame, CA). Staining was visualized by using an Olympus scanning confocal microscope (Olympus, Tokyo, Japan) at excitation/emission of 495/519 nm. The patch or macrodomain formation of Alexa488-labeled CTX and gangliosides complex represents the clusters of LRs. Clustering was defined as one or several intense spots or patches, rather than the diffusion of fluorescence on the cell surface, whereas a vast majority of unstimulated cells displayed a homogeneous distribution of fluorescence throughout the membrane. In each experiment, the presence or absence of clustering in samples of 200 cells was scored by unwitting researchers independently after specifying the criteria for positive spots of fluorescence. Cells displaying a homogeneous distribution of fluorescence were marked negative. Results were given as the percentage of cells showing one or more clusters after the indicated treatment as described.

Colocalization of LR clusters and NAD(P)H oxidase subunits or ASMase in CAECs

For dual-staining detection of the colocalization of LRs and NAD(P)H oxidase subunits, gp91^{phox}, p47^{phox}, or ASMase, the CAECs were first incubated with Alexa488-labeled CTX as described earlier and then with mouse anti-gp91^{phox} monoclonal antibody (BD Biosciences, San Jose, CA; 1:200), mouse anti-p47^{phox} monoclonal antibody (BD Biosciences; 1:200), or rabbit anti-ASMase polyclonal antibodies (Santa Cruz, Santa Cruz, CA; 1:200), separately, which was followed by Texas red–conjugated anti-mouse or anti-rabbit (Molecular Probes, Eugene, OR) secondary antibody as needed, respectively. An excitation/emission wavelength of 570/625 nm was used for confocal microscopy of Texas red.

Detection of lysosome trafficking to LR clusters in CAECs

For these experiments, CAECs were plated in a 35-mm dish (Nunclon, Raskilde, Denmark) at a density of 1×10^5 cells/ml and then cultured for 1 day. Living CAECs were loaded with 150 n*M* LysoTracker Red DND-99 (Molecular Probes) and 2

μg/ml Alexa488-conjugated CTX for 30 min. In additional groups of experiments, FasL, BAF, or GPN was added to the final concentrations indicated in individual experiments. After washing with PBS 3 times, the cells were visualized under a confocal microscope with an excitation wavelength of 577 nm and emission wavelength of 590 nm. In another group of cells, LysoTracker colocalization with CTX was detected after incubation of both staining markers in these living cells.

Measurements of reactive oxygen species (ROS) production in living CAECs

Detection of intracellular ROS was performed by a previously established method with a ROS-sensitive fluorescent probe, 2′,7′-dihydrodichlorofluorescin diacetate (DCF) and confocal microscopy (35). As described earlier, CAECs in 35-mm dishes were washed with PBS and loaded with 20 μM DCF (Molecular Probes) for 30 min at 37°C. The intensity of fluorescence of ROS-reactive dichlorofluorescin was quantified by using a laser-scanning confocal microscope (Olympus, Tokyo, Japan) with excitation and emission wavelengths of 488 and 520 nm, respectively.

ESR detection of $O_2^{\cdot -}$

ESR detection of $O_2^{\cdot -}$ was also performed, as we described previously (35). In brief, gently collected CAECs were suspended in modified Krebs/HEPEs buffer containing deferroximine (25 μM, metal chelator). Approximately 1×10^6 CAECs were mixed with 1 mM spin-trap 1-hydroxy-3-methoxycarbonyl-2,2,-5,5-tetrame-thyl-pyrrolidine (CMH) in the presence or absence of 100 units/ml polyethylene glycol (PEG)-conjugated superoxide dismutase (SOD). The cell mixture loaded in glass capillaries was immediately analyzed by ESR (Noxygen Science Transfer & Diagnostics GmbH, Denzlingen, Germany) for production of $O_2^{\cdot -}$ at each minute for 10 min. The ESR settings were as follows: biofield, 3,350; field sweep, 60 G; microwave frequency, 9.78 GHz; microwave power, 20 mW; modulation amplitude, 3 G; 4,096 points of resolution; receiver gain, 500; and kinetic time, 10 min. The SOD-inhibitable signals were normalized by protein concentration and compared among different experimental groups.

Isolated perfused small coronary artery preparation

Fresh bovine hearts were obtained from a local abattoir. Small coronary arteries (~200 μm ID) were prepared as we described previously (34). After dissection, arteries were transferred to a water-jacketed perfusion chamber and cannulated with two glass micropipettes at their *in situ* length. The outflow cannula was clamped, and the arteries were then pressurized to 60 mm Hg and equilibrated in physiologic saline solution (PSS, pH 7.4) containing (in mM): NaCl, 119; KCl, 4.7; $CaCl_2$, 1.6; $MgSO_4$, 1.17; NaH_2PO_4, 1.18; $NaHCO_3$, 2.24; EDTA, 0.026; and glucose, 5.5 at 37°C. PSS in the bath was continuously bubbled with a gas mixture of 95% O_2 and 5% CO_2 throughout the experiment. After a 1-h equilibration period, the arteries were precontracted by ~50% of their resting diameter with a thromboxane A_2 analogue, U-46619. Once steady-state contraction was obtained, cumulative dose–response curves to the endothelium-dependent vasodilator bradykinin (BK, 10^{-10}–10^{-6} M) were determined by measuring changes in internal diameter. In other groups of experiments, Baf or GPN was added into the lumen of the artery to preincubate for 15 min before the subsequent application of FasL. The vasodilator response was expressed as the percentage relaxation of U-46619–induced precontraction based on changes in arterial internal diameter. Internal arterial diameter was measured with a video system composed of a stereomicroscope (Leica MZ8), a charge-coupled device camera (KP-MI AU, Hitachi), a video monitor (VM-1220U, Hitachi), a video measuring apparatus (VIA-170; Boeckeler Instrument), and a video printer (UP890 MD, Sony).

Statistics

Data are presented as mean ± SEM. Significant differences between and within multiple groups were examined by using ANOVA for repeated measures, followed by Duncan's multiple-range test. A value of $p < 0.05$ was considered statistically significant.

RESULTS

Detection of LRs clustering and aggregated or recruited signaling molecules in the membrane of CAECs

As shown in Fig. 1, left panel, typical LR patches in a CAEC under resting condition and during FasL stimulation were de-

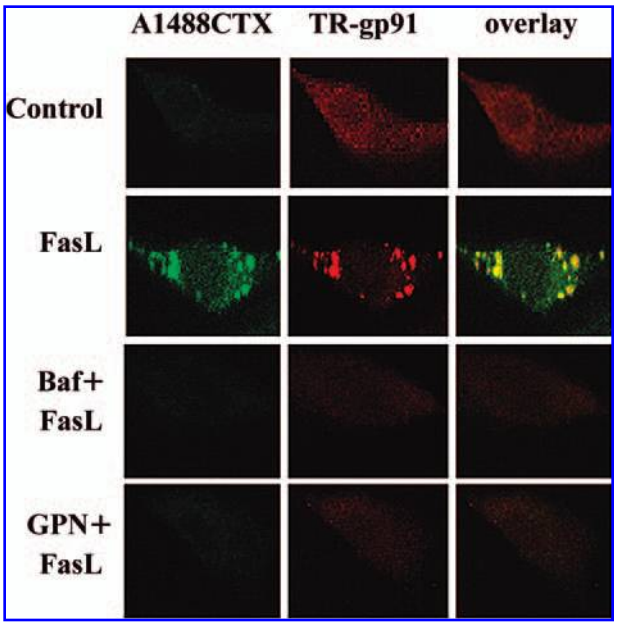

FIG. 1. Representative confocal microscopy of LR clusters (Alexa488-CTX green fluorescence at the left) and gp91^{phox} labeling (Texas red-conjugated anti-gp91^{phox} at the middle). The overlay of two images exhibits yellow spots or patches (right), which represent LRs clustering or colocalization of gp91^{phox} and the LR component, ganglioside G_M1.2.

tected by confocal microscopy. Under resting condition (control), only a diffuse fluorescent staining was observed on the cell membrane, indicating possible distribution of single LRs. However, when these cells were incubated with FasL, some large fluorescent dots were shown on the cell membrane, indicating LR patches or macrodomains. In the presence of either Baf or GPN, however, FasL-induced formation of LR clusters was substantially attenuated, and in many cells, no LR patches were detectable.

In the middle panel of Fig. 1, the cell stimulated by FasL was scanned with an excitation/emission of 570/625 nm for Texas red, which was conjugated to secondary antibody against anti-gp91^{phox} primary antibody. Red fluorescence indicated gp91^{phox} positive. In addition to some diffuse signals under resting conditions, relatively intense staining was found on the cell membrane of the cell stimulated by FasL. When two sequentially scanned images from the same cell with different wavelengths were merged, a number of yellow areas were noted, either as dots or as patches resulting from green CTX and Texas red-antiboby (right panel). These yellow patches were considered the colocalization of LR clusters and related molecules recognized by specific antibody. In this case, NAD(P)H oxidase subunit gp91^{phox} was the molecule colocalized with LR clusters. When the cells were pretreated by either Baf or GPN, both CTX clusters and aggregated Texas red fluorescence were no longer observed, and no co-staining of CTX and gp91^{phox} was seen.

Quantified LR clusters and its colocalization with NAD(P)H oxidase subunits or ASMase

For quantitative detection of LR clusters, CAECs were stained only with Alexa488-CTX, which could allow a more precise count of the large LR patches compared with double-staining. The results for these experiments are summarized in Fig. 2A. It was found that even control CAECs displayed a small percentage of cells with LRs clustering (9.3 ± 1.3%). After CAECs were stimulated with FasL, LRs-clustering positive cells increased significantly to 73.3 ± 8.4%; $p < 0.05$; $n = 6$). When Baf or GPN was used to pretreat cells, the FasL-induced increase in LRs-clustering positive cells was significantly reduced to 13.8 ± 1.7%, or 16.6 ± 3.1%, respectively. Figure 2B summarizes the results of doubled-stained CAECs by Alexa488-CTX and Texas red–conjugated gp91^{phox} antibody. These cells with yellow dots or patches after merging of fluorescent images with Alexa488 and Texas red indicated the colocalization of LR clusters and gp91^{phox}. In control CAECs, only about 5.5 ± 3.3% cells displayed colocalization of LR clusters and gp91^{phox}. After the cells were treated with FasL, the percentage of colocalization-positive cells significantly increased to 54.8 ± 9.2%. Consistent with the results from those cells stained by only CTX, pretreatment of CAECs with Baf or GPN significantly reduced the colocalization-positive cells to 9.5 ± 3.2% and 10.5 ± 4.3%, respectively. Figure 2C shows the summarized results of co-staining of CAECs with CTXB and anti-

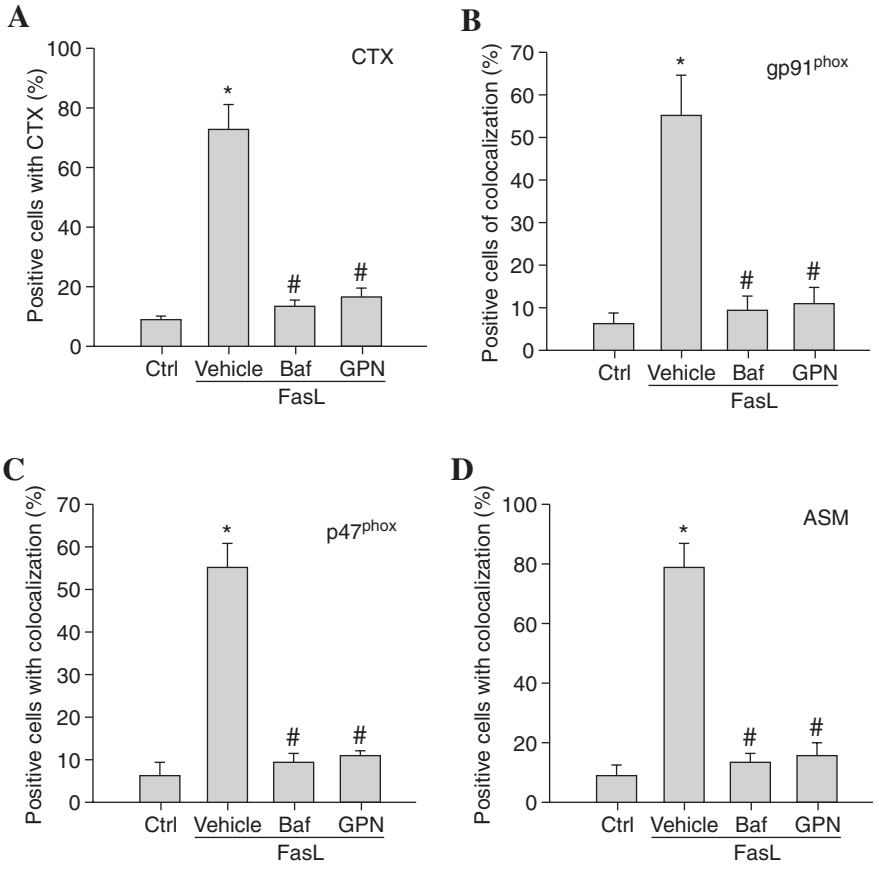

FIG. 2. Quantitative detection of LR clusters and colocalization of NAD(P)H oxidase subunits or ASMase in CAECs stimulated by FasL. (**A**) Percentage changes in positive cells stained by CTX during FasL stimulation with or without pretreatment by Baf or GPN. (**B**) Percentage changes in positive cells co-stained by CTX and anti-gp91^{phox} antibody during FasL stimulation with or without pretreatment by Baf or GPN. (**C**) Percentage changes in positive cells co-stained by CTX and anti-p47^{phox} antibody during FasL stimulation with or without pretreatment by Baf or GPN. (**D**) Percentage changes in positive cells co-stained by CTX and anti-ASMase antibody during FasL stimulation with or without pretreatment by Baf or GPN. The values in all panels are expressed as mean ± SEM over 1,000 cells. (*$p < 0.05$ vs. control; #$p < 0.05$ *vs*. FasL group; $n = 6$ primary cultures of CAECs.)

P47^{phox}. Compared with control, the percentage of colocalization-positive cells in FasL-stimulated group increased significantly (51.8 ± 9% *vs*. 6.5 ± 3.1%; $p < 0.05$; $n = 6$). When the cells were pretreated with Baf or GPN, the percentage of colocalization-positive cells, even in the presence of FasL, decreased to 8.5 ± 3.5% and 8.8 ± 3.3%, respectively. Figure 2D shows the percentage of colocalization-positive cells in double-staining experiments with CTX and anti-ASMase. Similarly, FasL induced a significantly increase in colocalization-positive cells, whereas after the cells were pretreated with Baf or GPN, Fas L no longer significantly increased colocalization-positive cells.

Association of LR clusters and lysosomal vesicles in living cells

By using LysoTracker as a lysosome marker, we determined the association of LRs clustering with lysosomal vesicles. Given that LysoTracker is designed to detect pH-related function of lysosomal vesicles in living cells, we first used a confocal microscope to examine whether time-dependent movements of lysosomal vesicles occur toward the cell membrane. However, we failed to observe obvious physical movements of lysosomal vesicles in these CAECs stimulated by FasL, even with a frequent acquisition of fluorescent images every 2 s over a 15-min period, including before and after the cells were treated with FasL (Fig. 3).

However, when a double staining of these CAECs with LysoTracker and Alexa488-CTX was examined, images of the cells exposed to FasL that were obtained by sequential scanning with LysoTracker wavelengths and Alexa488 wavelengths showed that FasL did not induce detectable increases or decrease in lysosomes (Fig. 4, middle panel). However, CTX staining significantly increased when the cells were incubated with FasL (Fig. 4, left panel). By merging two images, yellow areas were detected in response to FasL stimulation, suggesting possible colocalization of lysosomal vesicles with LR clusters (Fig. 4, right panel). In CAECs pretreated with Baf or GPN, however, lysosome staining by LysoTracker was substantially attenuated, accompanied by blockade of LRs clustering on the cell membrane, as shown in those images with labels of Baf+FasL and GPN+FasL. The quantitative percentage of LR cluster–positive cells is shown in Fig. 5. Similar to that observed in fixed cells, after stimulation by FasL, the percentage of LR cluster–positive cells significantly increased (80.8 ± 2.8% *vs*. 11.5 ± 3.1%; $p < 0.05$; $n = 6$); when Baf and GPN were used prior to FasL treatment, the percentage significantly decreased to 14.0 ± 1.8% and 13.5 ± 1.9%, respectively.

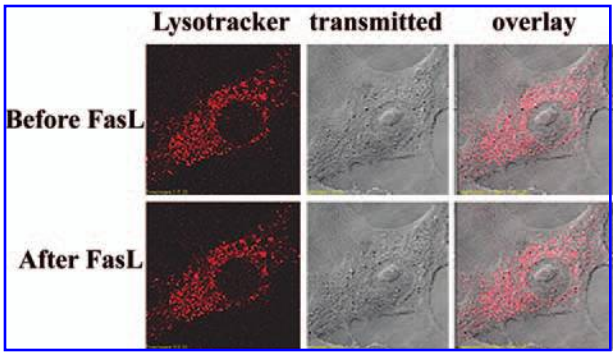

FIG. 3. Detection of lysosome movement before and after FasL stimulation. After loading with LysoTracker, the CAECs were underwent a highly frequent acquisition of fluorescent images every 2 s over a 15-min period, including before and after the cells were treated with FasL. The location of lysosomes in the cell before and 15 min after FasL stimulation is shown. This was repeatedly observed in four separate experiments.

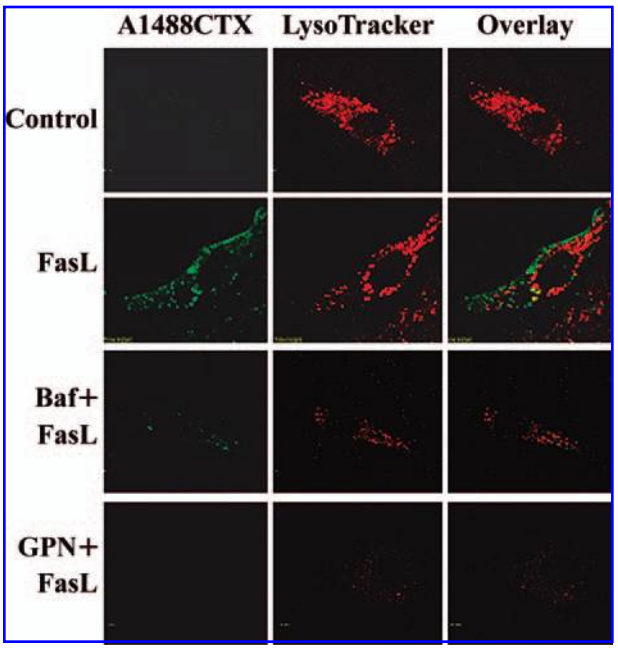

FIG. 4. Association of LR clusters and lysosomal vesicles in live CAECs. Representative images were obtained by confocal microscopy with LR marker Alexa488-CTX on the left (green) and colocalization of lysosomal vesicles labeled by LysoTracker (red). The overlay of two images exhibits yellow patches (*right*), which represent colocalization of lysosomal vesicles and LRs. This was consistently observed in six batches of primary cultures of CAECs.

Effects of Baf and GPN on FasL-induced $O_2^{\cdot -}$ production

The direct consequence of the activation of NAD(P)H oxidase is increased production of $O_2^{\cdot -}$. In Fig. 6A, typical ESR spectra were shown as SOD-inhibitable $O_2^{\cdot -}$ signals, and the amplitude in each spectrum reflected the signal intensity. FasL increased the amplitude of this SOD-inhibitable signal, as shown by increases in amplitude. In the presence of Baf or GPN, FasL no longer increased the amplitude of ESR spectra. Figure 6B presents the summarized data showing the fold changes of $O_2^{\cdot -}$ production. After these CAECs were treated with FasL, the $O_2^{\cdot -}$ level detected increased significantly. When the cells were pretreated with Baf or GPN, this FasL-induced increase in $O_2^{\cdot -}$ production was significantly reduced.

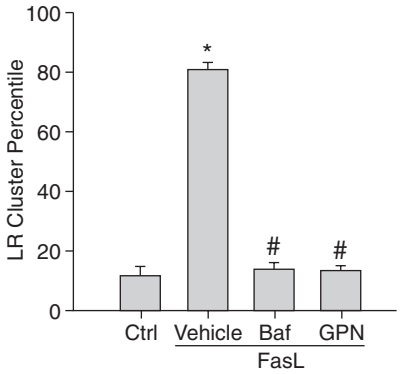

FIG. 5. Quantitative detection of LR clusters stimulated by FasL in live CAECs. This summarizes the percentage changes in live cells stained by CTX during FasL stimulation with or without pretreatment with Baf or GPN. (*$p < 0.05$ vs. control; #$p < 0.05$ vs. FasL group; $n = 6$ primary cultures of CAECs.)

Effects of Baf and GPN on FasL-stimulated ROS production in single CAECs

Because the ESR measurements described earlier could detect $O_2^{\cdot -}$ only from bulk-prepared cell lysates, it could not detect the production of $O_2^{\cdot -}$ in single cells. Further experiments were done to measure the production of ROS through lysosome-associated mechanism in single living cells. DCF was loaded into the cells, and then a rapid response of ROS production to FasL was observed. Figure 7A displays the dynamic changes in ROS production that was trapped by DCF. The intensity of DCF was quantitated to reflect the level of ROS within CAECs. In each group of cells, the fluorescence at a time point of 0, 1, 3, and 5 min was quantitated from acquired images. As summarized in Fig. 7B, in nonstimulated CAECs, the fluorescence intensity increased slightly over the experimental period. After FasL was added, however, the fluorescence intensity within individual cells significantly increased in a time-dependent manner. When the cells were pretreated with Baf or GPN, the FasL-induced increase in the fluorescence intensity was significantly attenuated, which was at a level similar to that obtained from those cells without FasL stimulation.

Reversal of FasL-induced impairment of endothelium-dependent vasodilation by Baf or GPN

Endothelium-dependent vasodilation induced by BK was determined in isolated perfused small bovine coronary arteries before and after FasL treatment. Figure 8 shows that BK produced a concentration-dependent increase in internal diameter of these small coronary arteries. Incubation of the arteries with FasL (10 ng/ml perfused into the lumen) had no significant effect on the basal arterial diameters, but markedly attenuated the BK-induced increase of arterial diameters. The inhibitory effect of FasL was reversed by a 15-min preincubation of the arteries with Baf or GPN. However, treatment of the arteries with Baf or GPN alone had no significant effect on basal arterial diameters or BK-induced vasodilation at the same doses used in the group of arteries treated with FasL. By transferring the dilation percentage into inhibition degree to the maximal dilation, FasL was found significantly to attenuate the coronary vasodilator response to BK, with an inhibition degree of 52.6% at the maximal dose of BK used in this study. When these arteries were pretreated with Baf or GPN, the inhibition action of FasL on BK-induced vasodilation was reduced to 2.1% and 11.4%, respectively.

DISCUSSION

In the present study, we examined the role of lysosomal vesicles in mediating FasL-induced formation of LR-redox signal-

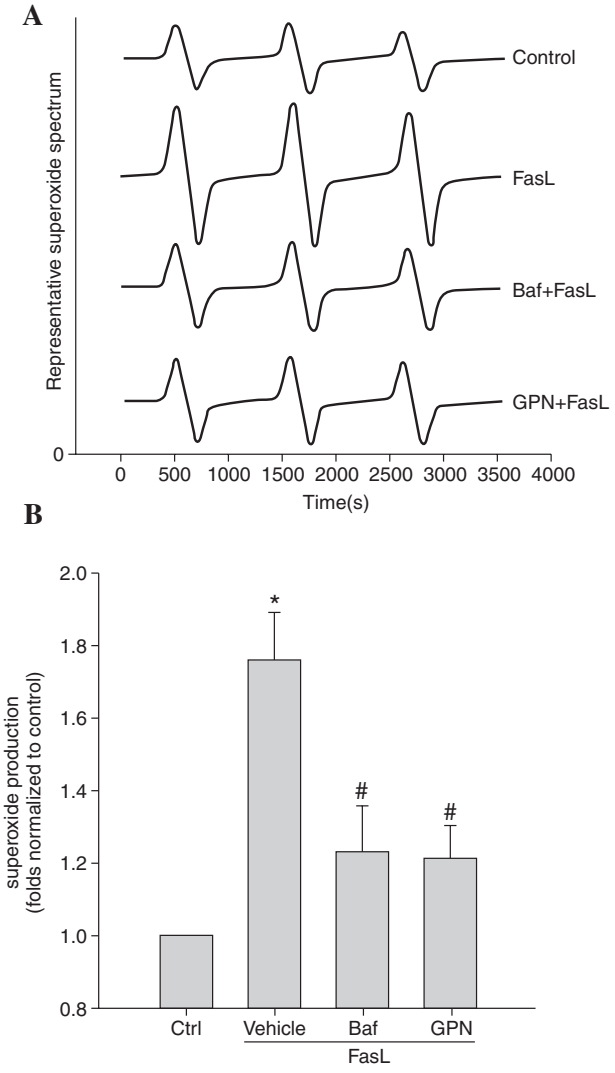

FIG. 6. Effects of Baf or GPN on FasL-induced $O_2^{\cdot -}$ production within CAECs. (**A**) Representative ESR spectra showing SOD-inhibitable $O_2^{\cdot -}$ signals. (**B**) Summarized data depicting changes in $O_2^{\cdot -}$ production in CAECs with different treatments (*$p < 0.05$ *vs.* control; #$p < 0.05$ *vs*. FasL group; $n = 5$).

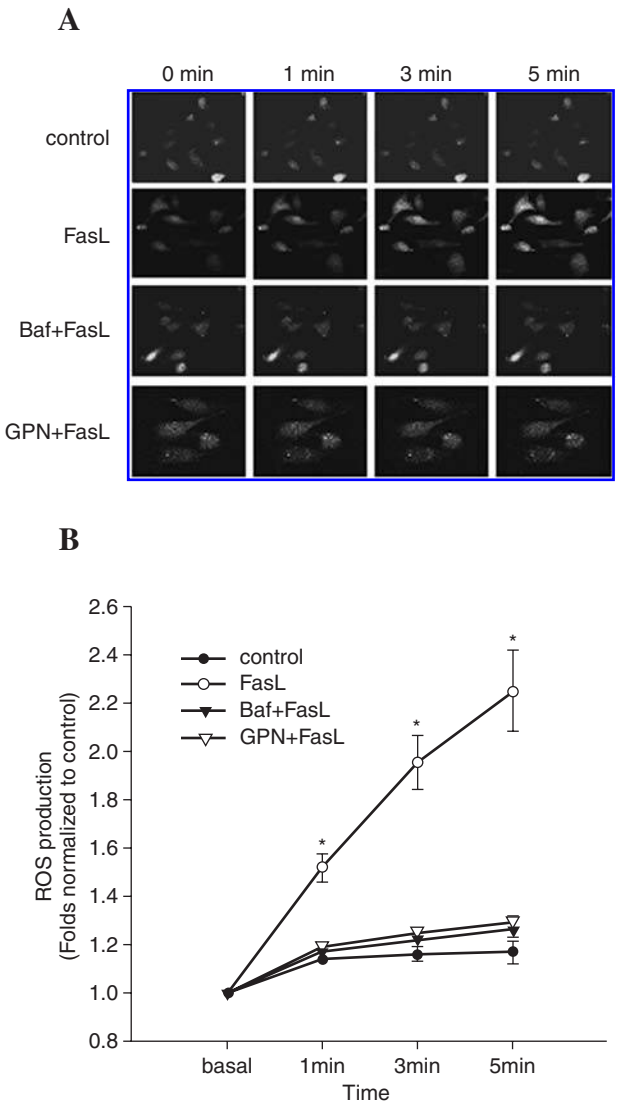

FIG. 7. Effects of Baf and GPN on FasL-induced ROS production within single CAECs. (**A**) Representative DCF fluorescent images showing dynamic changes in ROS levels within CAECs. (**B**) Summarized data depicting dynamic changes in ROS production in CAECs at an early time of FasL stimulation when the cells were treated with Baf or GPN. (*$p < 0.05$ *vs*. control; #$p < 0.05$ *vs*. FasL group; $n = 6$.)

ing platforms in the coronary artery EC membranes and corresponding changes in endothelial function in these arteries. By using two structurally different lysosomal vesicle inhibitors, Baf and GPN, we successfully blocked FasL-induced formation of LRs clustering and aggregation of NAD(P)H oxidase subunits in these LR clusters of CAECs, which resulted in significant reduction of FasL-induced ROS production. In isolated perfused small coronary arteries, FasL-induced impairment of vasodilator response to BK was also abolished by both vesicle inhibitors. These results strongly support the view that lysosomal vehicles contribute to the formation of LR redox signaling platforms in CAECs and thereby participate in the regulation of NAD(P)H oxidase activity and endothelial function in coronary arteries.

The major goal of the present study was to determine whether and how lysosomal vesicles are involved in the formation of LR redox signaling platforms and thereby regulate endothelial function. Lysosomes are membrane-bound organelles that originate from the Golgi apparatus and exist in the cytoplasm of all eucaryotic cells. These cytoplasmic organelles contain several dozens of acid hydrolases that are primarily responsible for intracellular digestion (5). With their intracellular digestion function, lysosomes can operate enzymatic digestion of endocytosed materials (cell defense) and aged organelles (cell autophagy) (7). They also play important roles in receptor-mediated endocytosis and mediate events of receptor recycling (20). More recently, lysosomal vesicles have been demonstrated to be responsible for exocytosis in nonsecretory cells (18), where these vesicles can fuse with the plasma membrane to excrete the contents of the vesicle and to incorporate the vesicle membrane components into the cell membrane (18). This lysosomal vesicle fusion to the cell membrane may be importantly involved in ASMase translocation in the process of LRs clustering, because this enzyme is present primarily in the lysosomal membrane, and on stimulation, it can be detected in the outer leaflet of the cell membrane (11). To determine directly whether lysosomes or their function contribute to LRs clustering and consequent formation of membrane signaling platforms, we first examined the effects of lysosome-function inhibition on death factor–induced formation of LR redox signaling platforms associated with the aggregation of NAD(P)H oxidase subunits. FasL was used in these experiments because previous studies demonstrated that it is one of the most potent death factors to induce LRs clustering and activation of NAD(P)H oxidase (6, 32). With a commonly used nontoxic cholera toxin subunit B (CTX-B) as a marker of LRs (2), FasL was found to stimulate

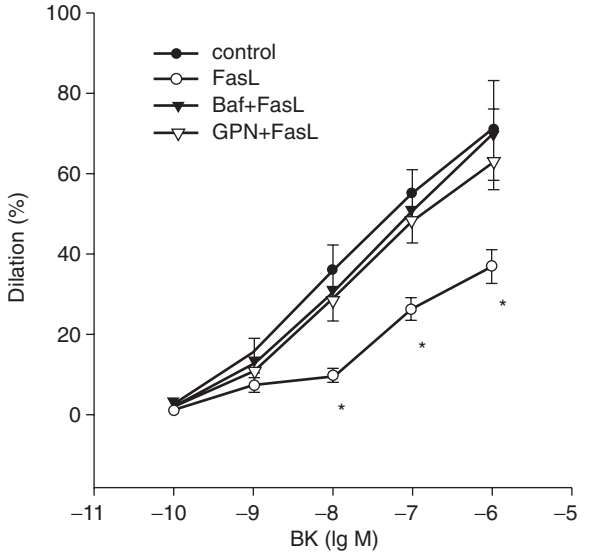

FIG. 8. Effects of Baf and GPN on FasL-induced impairment of endothelium-dependent vasodilation to BK in isolated perfused small coronary arteries. *$p < 0.05$ *vs*. control; $n = 5$ bovine hearts.

markedly the formation of LR clusters in bovine CAEC membrane (Figs. 1 and 2), which was consistent with previous results (32, 33). This FasL-stimulated LRs clustering was accompanied by aggregation of NAD(P)H oxidase subunits, gp91^{phox}, and recruitment of p47^{phox}, constituting a redox signaling platform. Two mechanistically different lysosomal vesicle inhibitors, Baf and GPN, substantially blocked LRs clustering and accompanied aggregation or recruitment of NAD(P)H oxidase subunits, suggesting that this redox molecule–associated LRs clustering is dependent on the integrity of lysosomal structure or function.

It has been reported that Baf is a macrolide antibiotic that specifically inhibits vacuolar H^+-ATPase (V-H^+-ATPase), resulting in a failure to pump protons into the lysosomal lumen for acidification (3). Decreased acidification of the lysosomal lumen has been shown to lead to loss of many lysosome functions, as listed earlier. Most important, Baf-damaged exocytosis and fusion of lysosomal membrane into the cell membrane might block translocation of ASMase into the cell membrane and thereby decrease ceramide production, plaguing LRs clustering associated with NAD(P)H oxidase. Indeed, we observed a reduced ASMase colocalized with LR clusters in these ECs. However, evidence exists that V-H^+-ATPase is present not only in lysosomes or lysosome-related vesicles, but also in the plasma membrane of certain cells such as endothelial cells (29). It is a concern whether the effects of Baf observed in the present study are associated with the inhibition of this plasma membrane V-H^+-ATPase. Although recent studies have demonstrated that Baf-inhibitable V-H^+-ATPase activity is expressed only in microvascular ECs, rather than in macrovascular ECs (22), such as we used in the present study, we performed further experiments to address this concern.

Using another mechanistically different inhibitor of lysosome function, GPN, the role of lysosomal vesicles in FasL-induced LRs clustering associated with NAD(P)H oxidase subunits was determined. GPN as a substrate of lysosomal cathepsin C may be hydrolyzed, and its hydrolysis products could be accumulated in the vesicle, resulting in a reversible osmotic swelling, and in this way interfering with lysosomal functions (1). As shown in Figs. 1 and 2, GPN was shown to inhibit FasL-induced LRs clustering and colocalization of gp91^{phox} and p47^{phox}, which was similar to that observed in Baf-treated cells. Correspondingly, GPN also blocked an accumulation of ASMase in the LR clusters (Fig. 2D). These results further confirm that lysosomal vesicles do participate in the formation of LR clusters with NAD(P)H oxidase subunits. The translocation of lysosomal ASMase may be of importance in this lysosome-related LRs clustering.

Further to explore the role of lysosomal vesicles in the formation of FasL-induced LR redox signaling platforms, we performed additional experiments to assess the movement of lysosomal vesicles to the cell periphery after stimulation with FasL in living bovine CAECs by using confocal microscopy with LysoTracker as a probe. LysoTracker is a fluorescent acidotropic probe for labeling and tracking lysosomal acidic organelles and has been widely used in studying trafficking of lysosomal vesicles within various cells DIN (25, 30). However, even with a very frequent acquisition of confocal fluorescent images, we could not detect obvious trafficking of lysosomal vesicles to the cell periphery in response to FasL stimulation. Given that LysoTracker stains primarily the intact lysosomal vesicles with a luminal acidic environment, these direct observations of vesicle numbers by only using LysoTracker may not reflect the dynamic changes in these vesicles under cell membrane because some vesicles trafficking to membrane might be broken and fused and therefore could not be detected by single LysoTracker staining.

To explore this possibility, we further performed live cell experiments with double staining of cells with LysoTracker and Alexa488-CTX. It was found that FasL stimulation of CAECs resulted in enhanced colocalization of LysoTracker-stained lysosomal vesicles and Alexa488-CTX–labeled ganglioside $G_M1.2$, indicating that on stimulation, lysosomal vesicles are closer to membrane components or LRs, where they may fuse and incorporate ASMase into the cell membrane, promoting ceramide production and formation of LR platforms. This ASMase relocation and ceramide production in the cell plasma membrane has been reported in a number of previous studies (2). In addition, the colocalization of lysosomal vesicles and LR components was significantly blocked by treatment with Baf and GPN, further suggesting that functional lysosomal vesicles are present in the proximal sites to LRs.

These lysosomal vesicles may interact with the cell membrane when the cells are stimulated by certain factors such as FasL. In previous studies, lysosomal displacement to the cell periphery was indicated as a mechanism to facilitate increased secretion of degradative enzymes such as matrix metalloproteinases, serine proteases, and cathepsins that are sequestered in lysosomal vesicles. This trafficking of lysosomal vesicles would be the first step in the recruitment of lysosomes toward the cell surface before lysosomal exocytosis (10, 24). However, this displacement of lysosomal vesicles is often observed in some cells subject to brief or relatively long stimulation (25, 30). Because we attempted to examine the early mechanism by which LR redox signaling platforms are formed in response to activation of death receptors, a relatively short exposure of cells to death factors such as FasL was used in our experiments. Therefore, the role of lysosomal vesicles in LRs clustering observed under this experimental condition may be attributed mainly to those vesicles in the proximity of cell membrane. Nevertheless, a trafficking of lysosomal vesicles in these CAECs during a brief or long-term treatment of FasL could not be excluded.

Next, we examined whether lysosomal vesicles contribute to the production of $O_2^{\cdot -}$ from LR platforms with NAD(P)H oxidase subunits. CAECs were stimulated by FasL in the absence and presence of Baf or GPN, and then intracellular $O_2^{\cdot -}$ production was detected by ESR spectrometry. In the absence of Baf or GPN treatment, FasL significantly increased $O_2^{\cdot -}$ production in CAECs. However, this FasL-induced $O_2^{\cdot -}$ production was markedly reduced when the cells were treated by either Baf or GPN. These results indicate that LRs clustering during FasL stimulation is indeed accompanied by activation of NAD(P)H oxidase. Although these experiments could not make sure that $O_2^{\cdot -}$ production in response to FasL is from cell-membrane LR platforms, our previous studies demonstrated in the same experimental condition that activation of NAD(P)H oxidase during FasL stimulation occurred mainly in LR membrane fractions (32). In addition, we monitored a dynamic change in $O_2^{\cdot -}$ level in single cells by fluorescent imag-

ing analysis of ROS within the cells. It was shown that, even at the first minute after FasL stimulation, ROS within CAECs were significantly increased. Pretreatment of these cells with either Baf or GPN completely blocked increases in intracellular $O_2^{\cdot -}$ levels. It appears that lysosomal vesicles are involved in the activation of NAD(P)H oxidase, which was consistent with the time course of the LRs clustering formation in response to FasL stimulation (10–20 s), as demonstrated in previous studies (13, 17). The results from a more recent study that endosomal acidification through V-H^+-ATPase during Fas activation enhanced ceramide formation and activation of NAD(P)H oxidase also support the possible interactions of lysosome-related vesicles and NAD(P)H oxidase activity (21). Taken together, these findings provide evidence that lysosomal vesicles importantly contribute to the activation of NAD(P)H oxidase through ceramide production and consequent formation of LR platforms.

The functional significance of this lysosomal vesicles–mediated formation of LR signaling platforms and activation of NAD(P)H oxidase was tested by measurement of endothelium-dependent vasodilation in isolated perfused small coronary arteries. It has been reported that endothelium-dependent vasodilation represents an early functional change in response to activation of death-receptor activation (31–33). In those studies, the role of LR clusters, ceramide, ASMase, and NAD(P)H oxidase in mediating endothelial dysfunction induced by various death factors was demonstrated. The present study further addressed whether lysosomal vesicles are also involved in the impairment of endothelial function associated with death-receptor activation. Similar to our previous studies (32, 33), FasL was found significantly to attenuate coronary vasodilator response to BK, a potent endothelium-dependent vasodilator in coronary circulation. When these arteries were pretreated with Baf or GPN, the blunting action of FasL on BK-induced vasodilation was almost completely blocked. This provides clear evidence that the functional integrity of lysosomal vesicles in the coronary arterial endothelium is important to the action of FasL on endothelial function. Based on the results discussed earlier regarding the role of lysosomal vesicles in the formation of LR redox signaling platforms and activation of NAD(P)H oxidase, we believe that failure of FasL to cause early endothelial dysfunction in Baf- or GNP-treated arteries may be associated with less production of $O_2^{\cdot -}$ production from the LR clustered NAD(P)H oxidase complex. Although the effect of NADPH oxidase inhibitor on the FasL-induced dilatation response were not directly tested, in a previous study (32) from our group, we confirmed this action of NADPH oxidase inhibitors to the FasL-induced impairment of vasodilation, which together supports the action of NADPH oxidase–derived ROS in this process. The role of this reduced production of $O_2^{\cdot -}$ in improvement of endothelial function during activation of death receptors has been shown in several of our previous studies (31–33) and by others (4, 8).

In summary, the present study demonstrated that lysosomal vesicles in the proximity of the cell membrane may play an important role in the formation of LR signaling platforms. If the integrity of lysosomal function or structure is lost, as shown in CAECs treated with Baf or GPN, LRs clustering and consequent aggregation or recruitment of NAD(P)H oxidase subunits could be blocked, thereby suppressing the actions of activated death receptors to transmit signals to downstream targets. This lysosomal vesicles–mediated formation and activity of LR redox signaling platforms may represent an important early mechanism responsible for endothelial dysfunction induced by death factors.

ACKNOWLEDGMENTS

This study was supported by grants from the National Institutes of Health (HL-57244, HL-75316, and DK54927). We thank Dr. Ningjun Li for his kindly help in writing the manuscript.

ABBREVIATIONS

DCF, 2′,7′-dihydrodichlorofluorescin diacetate; ASMase, acid sphingomyelinase; Baf, bafilomycin; BK, bradykinin; BSA, bovine serum albumin; CTXB, cholera toxin subunit B; CAECs, coronary artery endothelial cells; EGFR, epidermal growth factor receptor; FasL, Fas ligand; GPN, glycyl-L-phenylalanine-β-naphthylamide; LR, lipid raft; PFA, paraformaldehyde; PBS, phosphate-buffered saline; ROS, reactive oxygen species; SM, sphingomyelin; $O_2^{\cdot -}$, superoxide; TNFR, tumor necrosis factor receptor.

REFERENCES

1. Berg TO, Stromhaug E, Lovdal T, Seglen O, and Berg T. Use of glycyl-L-phenylalanine 2-naphthylamide, a lysosome-disrupting cathepsin C substrate, to distinguish between lysosomes and prelysosomal endocytic vacuoles. *Biochem J* 300: 229–236, 1994.
2. Bollinger CR, Teichgraber V, and Gulbins E. Ceramide-enriched membrane domains. *Biochim Biophys Acta* 1746: 284–294, 2005.
3. Bowman EJ, Siebers A, and Altendorf K. Bafilomycins: a class of inhibitors of membrane ATPases from microorganisms, animal cells, and plant cells. *Proc Natl Acad Sci U S A* 85: 7972–7976, 1988.
4. Cardier JE and Erickson-Miller CL. Fas (CD95)- and tumor necrosis factor-mediated apoptosis in liver endothelial cells: role of caspase-3 and the p38 MAPK. *Microvasc Res* 63: 10–18, 2002.
5. Cutler DF. Introduction: lysosome-related organelles. *Semin Cell Dev Biol* 13: 261–262, 2002.
6. Eramo A, Sargiacomo M, Ricci-Vitiani L, Todaro M, Stassi G, Messina CG, Parolini I, Lotti F, Sette G, Peschle C, and De Maria R. CD95 death-inducing signaling complex formation and internalization occur in lipid rafts of type I and type II cells. *Eur J Immunol* 34: 1930–1940, 2004.
7. Eskelinen EL. Roles of LAMP-1 and LAMP-2 in lysosome biogenesis and autophagy. *Mol Aspects Med* 27: 495–502, 2006.
8. Filippatos G, Ang E, Gidea C, Dincer E, Wang R, and Uhal BD. Fas induces apoptosis in human coronary artery endothelial cells in vitro. *BMC Cell Biol* 5: 6, 2004.
9. Furne C, Corset V, Herincs Z, Cahuzac N, Hueber AO, and Mehlen P. The dependence receptor DCC requires lipid raft localization for cell death signaling. *Proc Natl Acad Sci U S A* 103: 4128–4133, 2006.
10. Glunde K, Guggino SE, Solaiyappan M, Pathak AP, Ichikawa Y, and Bhujwalla ZM. Extracellular acidification alters lysosomal trafficking in human breast cancer cells. *Neoplasia* 5: 533–545, 2003.
11. Goggel R, Winoto-Morbach S, Vielhaber G, Imai Y, Lindner K, Brade L, Brade H, Ehlers S, Slutsky AS, Schutze S, Gulbins E, and Uhlig S. PAF-mediated pulmonary edema: a new role for acid sphingomyelinase and ceramide. *Nat Med* 10: 155–160, 2004.

12. Grassme H, Jekle A, Riehle A, Schwarz H, Berger J, Sandhoff K, Kolesnick R, and Gulbins E. CD95 signaling via ceramide-rich membrane rafts. *J Biol Chem* 276: 20589–20596, 2001.
13. Gulbins E and Kolesnick R. Acid sphingomyelinase-derived ceramide signaling in apoptosis. *Subcell Biochem* 36: 229–244, 2002.
14. Gupta N and DeFranco AL. Visualizing lipid raft dynamics and early signaling events during antigen receptor-mediated B-lymphocyte activation. *Mol Biol Cell* 14: 432–444, 2003.
15. Holopainen JM, Subramanian M, and Kinnunen PK. Sphingomyelinase induces lipid microdomain formation in a fluid phosphatidylcholine/sphingomyelin membrane. *Biochemistry* 37: 17562–17570, 1998.
16. Jury EC and Kabouridis PS. T-lymphocyte signalling in systemic lupus erythematosus: a lipid raft perspective. *Lupus* 13: 413–422, 2004.
17. Kirschnek S, Paris F, Weller M, Grassme H, Ferlinz K, Riehle A, Fuks Z, Kolesnick R, and Gulbins E. CD95-mediated apoptosis in vivo involves acid sphingomyelinase. *J Biol Chem* 275: 27316–27323, 2000.
18. Moreno RD and Alvarado CP. The mammalian acrosome as a secretory lysosome: new and old evidence. *Mol Reprod Dev* 73: 1430–1434, 2006.
19. Ni X and Morales CR. The lysosomal trafficking of acid sphingomyelinase is mediated by sortilin and mannose 6-phosphate receptor. *Traffic* 7: 889–902, 2006.
20. Nurminen TA, Holopainen JM, Zhao H, and Kinnunen PK. Observation of topical catalysis by sphingomyelinase coupled to microspheres. *J Am Chem Soc* 124: 12129–12134, 2002.
21. Reinehr R, Becker S, Braun J, Eberle A, Grether-Beck S, and Haussinger D. Endosomal acidification and activation of NADPH oxidase isoforms are upstream events in hyperosmolarity-induced hepatocyte apoptosis. *J Biol Chem* 281: 23150–23166, 2006.
22. Rojas JD, Sennoune SR, Maiti D, Bakunts K, Reuveni M, Sanka SC, Martinez GM, Seftor EA, Meininger CJ, Wu G, Wesson DE, Hendrix MJ, and Martinez-Zaguilan R. Vacuolar-type H+-ATPases at the plasma membrane regulate pH and cell migration in microvascular endothelial cells. *Am J Physiol Heart Circ Physiol* 291: H1147–H1157, 2006.
23. Rojas JD, Sennoune SR, Martinez GM, Bakunts K, Meininger CJ, Wu G, Wesson DE, Seftor EA, Hendrix MJ, and Martinez-Zaguilan R. Plasmalemmal vacuolar H+-ATPase is decreased in microvascular endothelial cells from a diabetic model. *J Cell Physiol* 201: 190–200, 2004.
24. Rozhin J, Sameni M, Ziegler G, and Sloane BF. Pericellular pH affects distribution and secretion of cathepsin B in malignant cells. *Cancer Res* 54: 6517–6525, 1994.
25. Sarnataro D, Grimaldi C, Pisanti S, Gazzerro P, Laezza C, Zurzolo C, and Bifulco M. Plasma membrane and lysosomal localization of CB1 cannabinoid receptor are dependent on lipid rafts and regulated by anandamide in human breast cancer cells. *FEBS Lett* 579: 6343–6349, 2005.
26. Sato K, Shikano S, Xia G, Takao J, Chung JS, Cruz PD Jr, Xie XS, and Ariizumi K. Selective expression of vacuolar H+-ATPase subunit d2 by particular subsets of dendritic cells among leukocytes. *Mol Immunol* 43: 1443–1453, 2006.
27. Schissel SL, Keesler GA, Schuchman EH, Williams KJ, and Tabas I. The cellular trafficking and zinc dependence of secretory and lysosomal sphingomyelinase, two products of the acid sphingomyelinase gene. *J Biol Chem* 273: 18250–18259, 1998.
28. Sprenger RR, Fontijn RD, van Marle J, Pannekoek H, and Horrevoets AJ. Spatial segregation of transport and signalling functions between human endothelial caveolae and lipid raft proteomes. *Biochem J* 400: 401–410, 2006.
29. Sun-Wada GH, Wada Y, and Futai M. Lysosome and lysosome-related organelles responsible for specialized functions in higher organisms, with special emphasis on vacuolar-type proton ATPase. *Cell Struct Funct* 28: 455–463, 2003.
30. Trajkovic K, Dhaunchak AS, Goncalves JT, Wenzel D, Schneider A, Bunt G, Nave KA, and Simons M. Neuron to glia signaling triggers myelin membrane exocytosis from endosomal storage sites. *J Cell Biol* 172: 937–948, 2006.
31. Zhang AY, Teggatz EG, Zou AP, Campbell WB, and Li PL. Endostatin uncouples NO and Ca^{2+} response to bradykinin through enhanced $O_2{}^{*-}$ production in the intact coronary endothelium. *Am J Physiol Heart Circ Physiol* 288: H686–H694, 2005.
32. Zhang AY, Yi F, Zhang G, Gulbins E, and Li PL. Lipid raft clustering and redox signaling platform formation in coronary arterial endothelial cells. *Hypertension* 47: 74–80, 2006.
33. Zhang AY, Yi F, Zhang G, Gulbins E, and Li PL. RNA interference of acidic sphingomyelinase gene restores endothelial function through inhibition of NAD(P)H oxidase activity. *FASEB J* 19: A521, 2005.
34. Zhang DX, Yi FX, Zou AP, and Li PL. Role of ceramide in TNF-alpha-induced impairment of endothelium-dependent vasorelaxation in coronary arteries. *Am J Physiol Heart Circ Physiol* 283: H1785–H1794, 2002.
35. Zhang G, Zhang F, Muh R, Yi F, Chalupsky K, Cai H, and Li PL. Autocrine/paracrine pattern of superoxide production through NAD(P)H oxidase in coronary arterial myocytes. *Am J Physiol Heart Circ Physiol* 292: H483–H495, 2007.

Address reprint requests to:
Pin-Lan Li, M.D, Ph.D.
Department of Pharmacology and Toxicology
Medical College of Virginia
Virginia Commonwealth University
410 N 12th, Richmond, VA 23298

E-mail: pli@vcu.edu

Date of first submission to ARS Central, March 27, 2007, date of final revised submission, March 27, 2007; date of acceptance, March 28, 2007.

This article has been cited by:

1. Ming Xu, Yang Zhang, Min Xia, Xiao-Xue Li, Joseph K. Ritter, Fan Zhang, Pin-Lan Li. 2011. NAD(P)H oxidase-dependent intracellular and extracellular O2•- production in coronary arterial myocytes from CD38 knockout mice. *Free Radical Biology and Medicine* . [CrossRef]
2. Si Jin , Fan Zhou , Foad Katirai , Pin-Lan Li . Lipid Raft Redox Signaling: Molecular Mechanisms in Health and Disease. *Antioxidants & Redox Signaling*, ahead of print. [Abstract] [Full Text] [PDF] [PDF Plus]
3. M. Xia, C. Zhang, K. M. Boini, A. M. Thacker, P.-L. Li. 2011. Membrane raft-lysosome redox signalling platforms in coronary endothelial dysfunction induced by adipokine visfatin. *Cardiovascular Research* **89**:2, 401-409. [CrossRef]
4. Qiao Yang, Hong Yan Liu, Yao Wen Zhang, Wen Jie Wu, Wang Xian Tang. 2010. Anandamide induces cell death through lipid rafts in hepatic stellate cells. *Journal of Gastroenterology and Hepatology* **25**:5, 991-1001. [CrossRef]
5. Jun-Xiang Bao , Si Jin , Fan Zhang , Zheng-Chao Wang , Ningjun Li , Pin-Lan Li . 2010. Activation of Membrane NADPH Oxidase Associated with Lysosome-Targeted Acid Sphingomyelinase in Coronary Endothelial Cells. *Antioxidants & Redox Signaling* **12**:6, 703-712. [Abstract] [Full Text] [PDF] [PDF Plus] [Supplementary Material]
6. Si Jin, Fan Zhou. 2009. Lipid raft redox signaling platforms in vascular dysfunction: Features and mechanisms. *Current Atherosclerosis Reports* **11**:3, 220-226. [CrossRef]
7. Pin-Lan Li , Erich Gulbins . 2007. Lipid Rafts and Redox Signaling. *Antioxidants & Redox Signaling* **9**:9, 1411-1416. [Abstract] [PDF] [PDF Plus]